

## Low-temperature transport properties of NdBiPt

Donald T. Morelli

*Physics Department, General Motors Research and Development Center, Warren, Michigan 48090-9055*

Paul C. Canfield and Phoebus Drymiotis

*Ames Laboratory and Department of Physics, Iowa State University, Ames, Iowa 50011*

(Received 26 October 1995)

NdBiPt is a member of a new class of ternary intermetallic semiconductors and semimetals. These materials are covalently bonded crystals with band gaps expected to be in the range of 0–1 eV. Longitudinal resistivity, Hall resistivity, and thermoelectric power measurements reveal that in NdBiPt the “gap” is an overlap that gives rise to a semimetallic behavior exhibiting high hole and electron mobilities. [S0163-1829(96)04119-7]

### INTRODUCTION

Interest in materials with complex crystal structures exhibiting unconventional or exotic electronic properties has flourished within the past decade. Oxide perovskites with high superconducting transition temperatures, doped lanthanum manganite with magnetically driven “colossal” magnetoresistance,<sup>1–3</sup> and skutterudite compounds with unusual transport properties<sup>4–6</sup> are just a few examples. Another recently discovered class of materials exhibiting unusual transport and optical properties are the ternary intermetallics of the form MNiSn (M=Ti, Zr, or Hf).<sup>7–10</sup> These properties seem to imply the existence of a gap at the Fermi level on the order of 0.1–0.2 eV. The MNiSn system is a subset of a larger family of compounds possessing the MgAgAs (AlLiSi) structure, of which over 100 different compounds are known.<sup>11</sup> Another series of this type of the form RBiPt, where R is a rare-earth element, has been recently examined in detail by Canfield *et al.*<sup>12</sup> These compounds exhibit a semiconductorlike rise in the electrical resistivity with decreasing temperature with an activation energy that decreases with increasing rare-earth atomic weight, eventually evolving into a heavy-fermion-like metallic state for YbBiPt.<sup>13,14</sup>

The origin of semiconducting behavior in a material consisting of good metals in a 1:1:1 ratio is an intriguing and challenging theoretical problem. The MgAgAs structure can be viewed as three face-centered-cubic sublattices placed at (0,0,0),  $(\frac{1}{4}, \frac{1}{4}, \frac{1}{4})$ , and  $(\frac{1}{2}, \frac{1}{2}, \frac{1}{2})$  along the body diagonal and thus is similar in some sense to the zinc-blende structure of III-V semiconductors in which the  $(\frac{1}{2}, \frac{1}{2}, \frac{1}{2})$  site is unoccupied. Recently, Ögüt and Rabe<sup>15</sup> performed total-energy and electronic band-structure calculations for MNiSn and predicted indirect gaps near 0.5 eV. Further, they attributed the structural stability of these compounds to the stability of the binary SnM substructure, while the opening of the gap is due to the symmetry-breaking Ni sublattice. In the case of NdBiPt (space group  $F\bar{4}3m$ ) the structure is more easily thought of as a “filled” variant of the rocksalt NdBi structure (space group  $Fm\bar{3}m$ ), where Nd and Bi are on the (0,0,0) and  $(\frac{1}{2}, \frac{1}{2}, \frac{1}{2})$  sites and the Pt “fills” the structure by going on the  $(\frac{1}{4}, \frac{1}{4}, \frac{1}{4})$  site. Thus the NdBiPt structure is fully ordered and of lower symmetry than the binary rocksalt

NdBi structure. In initial work<sup>12</sup> the crystallographic sites for the three elements were misidentified, but recent x-ray and neutron-scattering studies on RBiPt (Ref. 16) support the above picture and show no evidence of any site disorder in these compounds.

In this paper we report the preparation and low-temperature transport properties of NdBiPt, which as mentioned above possesses the MgAgAs structure. Our results indicate that this compound is a semimetal. The origin of this semimetallic behavior is discussed in terms of the Ögüt-Rabe picture of structural stability and semiconductivity of these compounds.

### EXPERIMENT

Single crystals of NdBiPt were grown from excess Bi flux as has been described by Canfield *et al.* in earlier papers.<sup>12,17</sup> The sample reported on here had the same room temperature resistivity ( $\rho \approx 0.95 \text{ m}\Omega \text{ cm}$ ) and relative increase (approximately tenfold) upon cooling to liquid-helium temperatures as those reported in Ref. 12; see Fig. 1. We have measured the magnetic susceptibility and longitudinal and transverse (Hall) resistivities of this single crystal, as well as the thermoelectric power of a larger twinned single crystal from the same growth. The magnetic susceptibility was measured using a Quantum Design superconducting quantum interference device magnetometer and the galvanomagnetic measurements were carried out from 4 to 300 K in the van der Pauw geometry using silver wires and silver epoxy contacts. Sample currents were kept below 10 mA to prevent sample heating and both current and field direction were reversed to eliminate the effects of thermal offsets and probe misalignment. Thermopower measurements were performed using a steady-state technique with Pb probes, the Seebeck coefficient of which was accounted for using the tables of Roberts.<sup>18</sup>

### RESULTS AND DISCUSSION

Figure 2 shows the inverse magnetic susceptibility (measured at 5000 G) of our NdBiPt single crystal as a function of temperature. The solid line is a fit to the data assuming Curie-Weiss behavior and yields an effective moment  $\mu_{\text{eff}} \approx 3.6\mu_B$ , indicating that the rare-earth ion is in the triva-

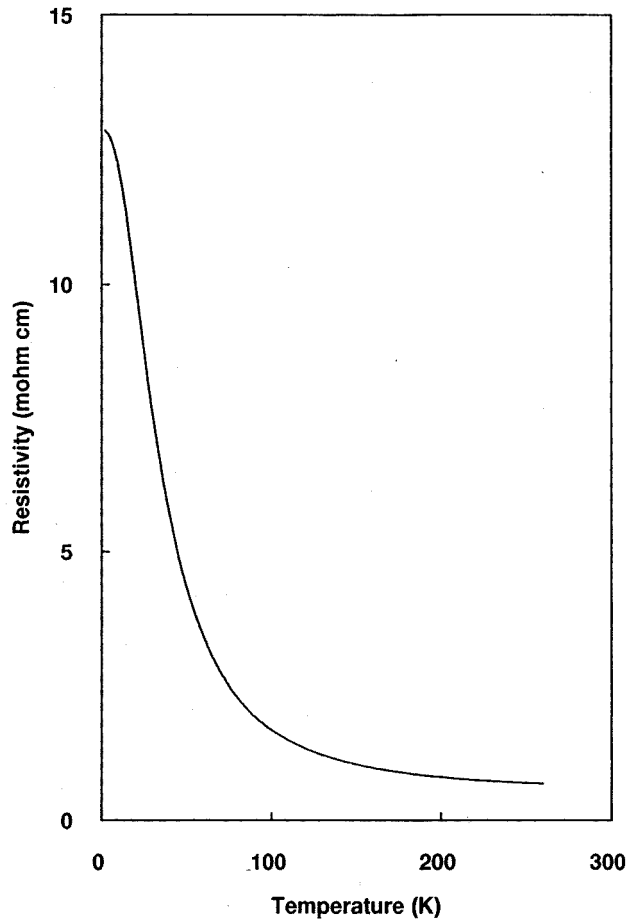


FIG. 1. Resistivity of a single crystal of NdBiPt.

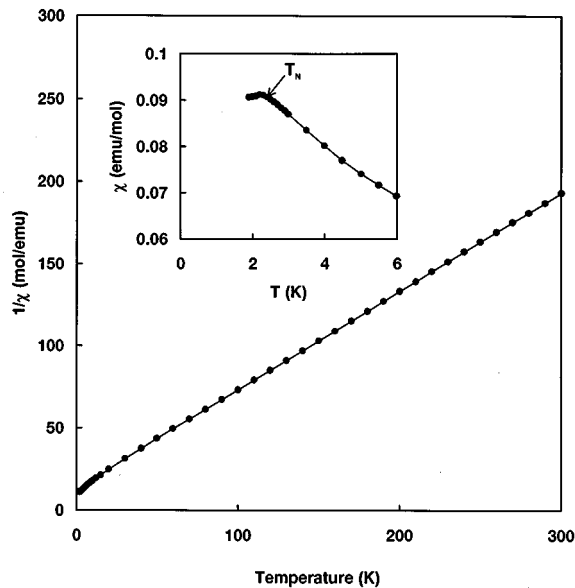


FIG. 2. Inverse susceptibility of NdBiPt as a function of temperature. The solid line is the Curie-Weiss behavior with  $\mu_{\text{eff}} \approx 3.6\mu_B$  and  $\theta \approx -23$  K. The inset shows the detail at low temperature and indicates the antiferromagnetic transition temperature  $T_N \approx 2.2$  K.

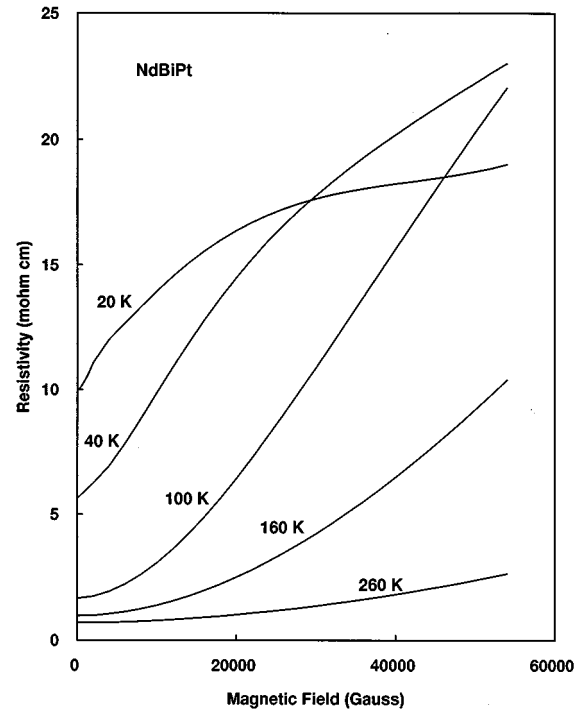


FIG. 3. Longitudinal resistivity  $\rho_{xx}(B)$  at selected temperatures for NdBiPt.

lent state, and a paramagnetic  $\theta \approx -23$  K in agreement with.<sup>12</sup> We also confirm the observation of Canfield *et al.*<sup>12</sup> of an antiferromagnetic phase transition at  $T_N \approx 2.2$  K; see the inset of Fig. 2.

Figures 3 and 4 exhibit the longitudinal ( $\rho_{xx}$ ) and transverse ( $\rho_{xy}$ ) electrical resistivities as a function of magnetic

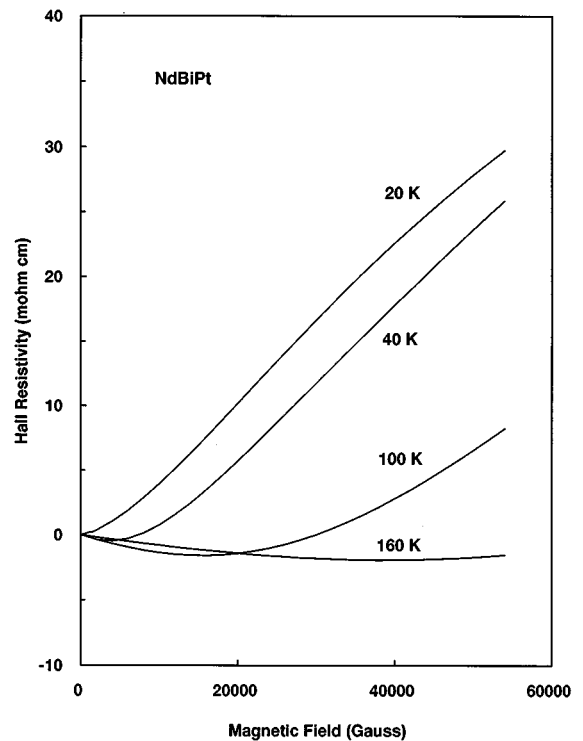


FIG. 4. Transverse (Hall) resistivity  $\rho_{xy}(B)$  at selected temperatures for NdBiPt.

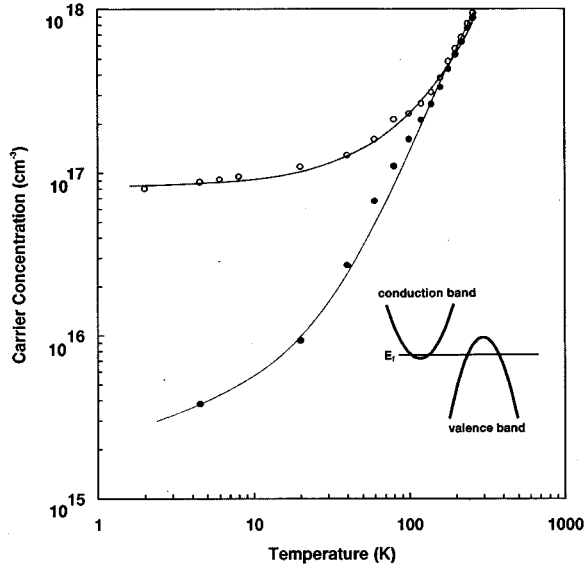


FIG. 5. Electron (●) and hole (○) concentrations as a function of temperature in single crystal NdBiPt, as determined from a two-band fit to  $\rho_{xx}$  and  $\rho_{xy}$ . Solid lines are fits to the data using Fermi-Dirac statistics, which yield Fermi energies of  $E_{Fh} \approx 5$  meV and  $E_{Fe} \approx 1$  meV.

field for selected temperatures. We note that the resistivity is strongly field dependent, exhibiting as much as a tenfold increase with field. The Hall resistivity is also strongly field and temperature dependent and even changes sign as a function of both of these variables. In particular, this sample appears to be  $n$  type at room temperature and  $p$  type at low temperature. It is quite clear from these results that this is a system with at least two types of carriers of opposite sign. We will assume that there are electrons of density  $n$  and mobility  $\mu$  and holes of density  $p$  and mobility  $\nu$  and adopt a two-band model to quantitatively model the data. In this picture one has for the longitudinal and transverse conductivities

$$\sigma_{xx} = ne\mu/(1 + \mu^2 B^2) + pe\nu/(1 + \nu^2 B^2),$$

$$\sigma_{xy} = ne\mu^2 B/(1 + \mu^2 B^2) + pe\nu^2 B/(1 + \nu^2 B^2).$$

The conductivities as a function of field are fit at each temperature using a least-squares routine with  $n$ ,  $p$ ,  $\mu$ , and  $\nu$  as adjustable parameters. The results of this procedure are plots of the carrier concentrations  $n$  and  $p$  and the carrier mobilities  $\mu$  and  $\nu$  as functions of temperature; see Figs. 5 and 6. We see that in NdBiPt we have both holes and electrons of high mobility (for comparison the electron mobilities in Si and GaAs at 300 K are 1500 and 8500  $\text{cm}^2 \text{V}^{-1} \text{s}^{-1}$ , respectively). Near room temperature the carrier concentrations are nearly equal, but the electron mobility is higher than the hole mobility, so the material appears to be  $n$  type. At low temperatures the hole concentration exceeds the electron concentration by an order of magnitude and this is sufficient to offset the mobility difference and make the material appear to be  $p$  type. The solid lines in Fig. 5 represent fits of the carrier densities assuming Fermi-Dirac statistics and yield hole and electron Fermi energies of  $E_{Fh} \approx 5$  meV and  $E_{Fe} \approx 1$  meV. The band scheme shown in the inset of Fig. 5 is con-

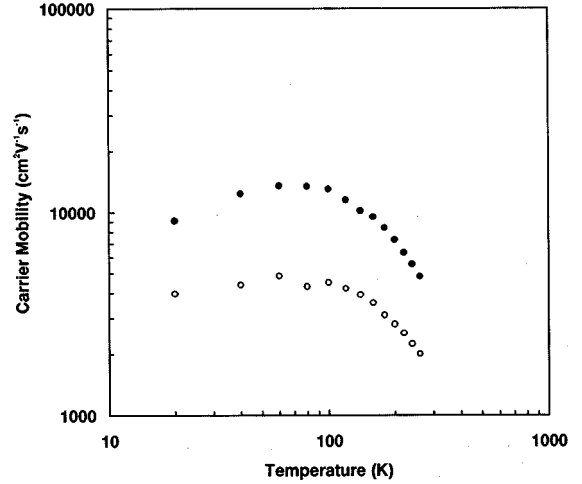


FIG. 6. Electron (●) and hole (○) mobilities as a function of temperature in single crystal NdBiPt, as determined from a two-band fit to  $\rho_{xx}$  and  $\rho_{xy}$ .

sistent with these Fermi energies and identifies NdBiPt as a semimetal with a very small overlap. If the material were a pure semimetal, we should have  $n = p$  at all temperatures. The fact that the hole concentration exceeds the electron concentration at low temperature indicates that the material is doped slightly  $p$  type, pushing the Fermi energy down lower into the valence band. Since the difference  $p - n$  is on the order of  $10^{17} \text{ cm}^{-3}$ , only a few ppm of impurity would be sufficient to produce this effect. Potential impurity sources that can account for this slight doping are impurities in the Pt, which was 99.9% pure, or simply site disorder on the ppm level.

While the resistivity versus field profiles are quadratic at high temperatures, the high-field resistivity bands over at high fields and low temperatures, with some interesting features developing below 10 K. In Fig. 7 we show the longitudinal resistivity versus  $B$  at 4.5 K. This curve is characterized by a shoulder near 0.6 T and a strong minimum near 4 T. While it is possible that this interesting structure is due to some magnetic effects, this seems unlikely since the sample is still in the paramagnetic state at this temperature, the phase transition not occurring until 2.2 K. We believe, rather, that this is a single Shubnikov-de Haas oscillation of period 1.35  $\text{T}^{-1}$ . Assuming a spherical Fermi surface, this corresponds to

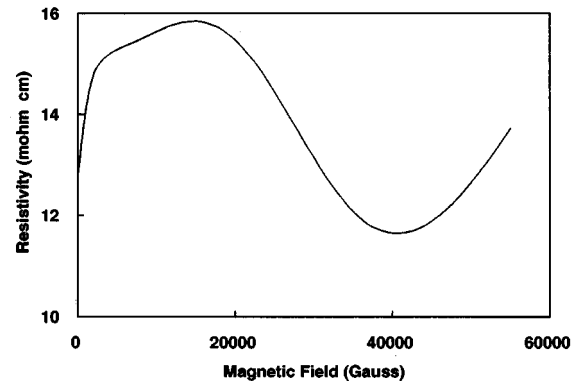


FIG. 7. Longitudinal resistivity  $\rho_{xx}$  at 4.5 K of NdBiPt.

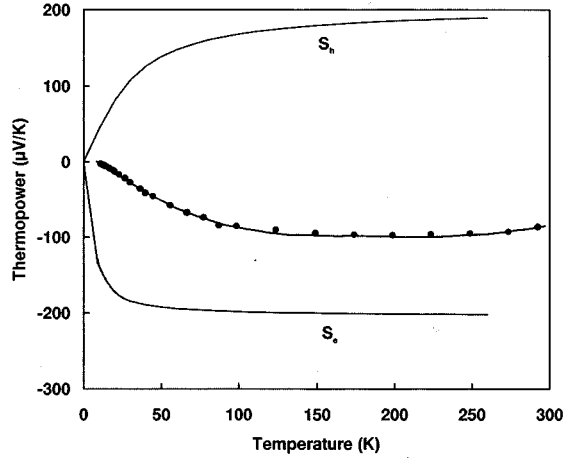


FIG. 8. Thermoelectric power of a NdBiPt twinned crystal.  $S_e$  and  $S_h$  are the partial electron and hole thermopowers, respectively, calculated from Fermi energies determined from the carrier concentrations of Fig. 5. The solid line through the data is a fit using the two-band model.

a carrier concentration of approximately  $3 \times 10^{15} \text{ cm}^{-3}$ , roughly what one would expect for the electron concentration at this temperature; see Fig. 5. Although the hole concentration is larger, which would correspond to a smaller Shubnikov–de Haas period, presumably they are not of high enough mobility to observe oscillations. de Haas–van Alphen oscillations in the electronic susceptibility are not observable due to the large paramagnetism of the  $\text{Nd}^{3+}$  ions.

Another manifestation of the semimetallic nature of this system and the contribution of both electrons and holes to the conduction process can be observed in the thermoelectric power; see Fig. 8. The thermoelectric power is negative throughout the entire temperature range and has a weak negative maximum near 200 K. We note however, that  $S(T)$  does not extrapolate to zero but rather appears to be approaching positive values were the data to extend below 10 K. Assuming acoustic phonon scattering, we can determine the partial hole and electron thermopowers from the Fermi energies derived from the galvanomagnetic data using the relations

$$S_e = -k/e[2F_1(\eta_e)/F_0(\eta_e) - \eta_e],$$

$$S_h = k/e[2F_1(\eta_h)/F_0(\eta_h) - \eta_h],$$

where  $\eta_{e,h} = E_{F_{e,h}}/kT$  and  $F_1$  and  $F_0$  are Fermi-Dirac integrals. The total thermopower is then given by  $S = (S_e \sigma_e + S_h \sigma_h)/(\sigma_e + \sigma_h)$ . In Fig. 8 we show a fit to the data using this expression with the partial conductivities as adjustable parameters and in Fig. 9 we show the partial electron and hole conductivities as a function of temperature so derived. These can be compared directly with those determined using  $\sigma_e = ne\mu$  and  $\sigma_h = pe\nu$  from the galvanomagnetic data for  $n$ ,  $p$ ,  $\mu$ , and  $\nu$ . As can be seen in Fig. 9, the agreement between the partial conductivities using these two independent methods is very good, especially in view of the fact that the thermopower and galvanomagnetic data were gathered on different samples. This lends strong support to the semimetal model for NdBiPt.

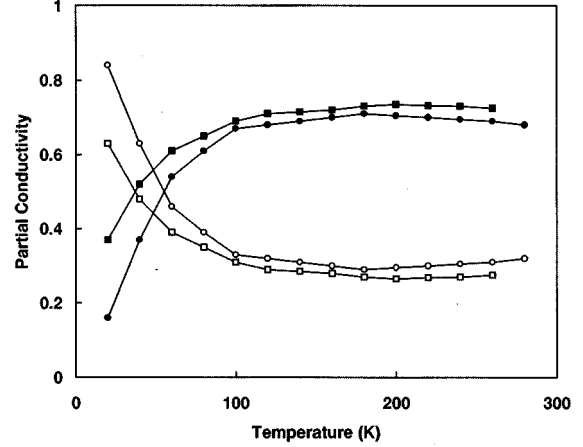


FIG. 9. Partial electron (solid symbols) and hole (open symbols) conductivities of NdBiPt: circles, as determined from galvanomagnetic measurements on single crystal; squares, as determined from thermopower measurements on a twinned single crystal.

It is interesting to speculate on the origin of semimetallicity of this compound. According to Ögüt and Rabe,<sup>15</sup> the essential features of the states near the Fermi level in the ternary  $\text{ZrNiSn}$  phase are determined by the atomic orbitals of the binary  $\text{SnZr}$  substructure. In the present case the relevant binary substructure is NdBi and the essential features of the band structure of NdBiPt should already be evident in the band structure of NdBi. In the latter, the five electrons from the pnictide  $p$  and  $s$  states together with the three valence electrons from the rare-earth atom provide the eight total electrons, which is just enough to fill the four-lowest-lying bands derived from the anionic (i.e., bismuth) hybridized orbitals. However, according to Honig<sup>19</sup> for the rare-earth pnictides such as NdBi, an overlapping of the highest anion-anion orbital at the  $\Gamma$  point in the Brillouin zone with the  $t_{2g}$  orbital derived from the rare-earth  $d$  states at the  $X$  point is expected to occur, causing partial occupation of the former by holes and the latter by electrons, and a semimetal results. A similar result was derived by Petukhov, Lambrecht, and Segall for ErAs.<sup>20</sup> Indeed, it is thought that most trivalent rare-earth–pnictide binary compounds, with the possible exception of the nitrides, are semimetals and that the overlap increases with increasing atomic weight.<sup>21</sup> To test this hypothesis, we have also grown single crystals of NdBi and measured their electrical transport properties. As can be seen in Fig. 10, NdBi is metallic with a room-temperature resistivity of approximately  $60 \mu\Omega \text{ cm}$ ; Hall measurements place a lower bound on the carrier concentration of  $1.2 \times 10^{21} \text{ cm}^{-3}$  (the feature in the resistivity at 24 K corresponds to an antiferromagnetic transition). Assuming a carrier mass equal to the free-electron value, this concentration corresponds to a Fermi energy of about 0.4 eV. In addition, Allen *et al.*<sup>22–24</sup> have recently demonstrated unequivocally that ErAs is a semimetal with  $n \approx p \approx 10^{20} \text{ cm}^{-3}$ . In going from the binary substructure of NdBi to the ternary NdBiPt, one would expect, in analogy with  $\text{ZrNiSn}$ , that the addition of Pt to the NdBi substructure would “increase the gap,” that is, decrease the overlap of the bands, and this may be the case since our experimental results for NdBiPt indicate only a very small overlap and concentrations of approximately  $10^{18} \text{ cm}^{-3}$ , two to three orders of magnitude less than

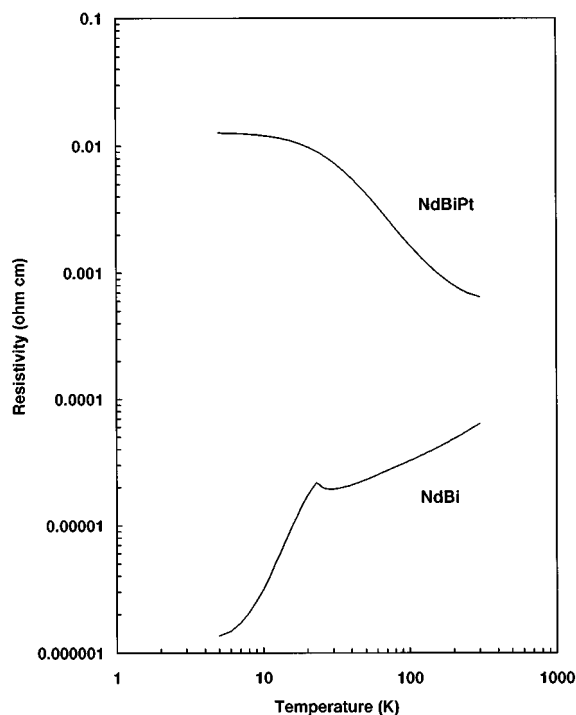


FIG. 10. Electrical resistivity of single crystals of NdBiPt and NdBi. The feature at 24 K in the resistivity of NdBi occurs at the magnetic ordering temperature.

the carrier concentrations in the binary compound NdBi. Further, more detailed, low-temperature measurements on high-quality single crystals of the binary substructure NdBi are presently being carried out to further elucidate the relationship between the ternary compound and its binary-substructure relative.

## CONCLUSIONS

We have carried out detailed measurements of the low-temperature transport properties of the ternary intermetallic NdBiPt, which possesses the MgAgAs structure. The results indicate that this compound is a semimetal with high electron and hole mobilities. In the framework of the model of Ögüt and Rabe,<sup>15</sup> developed for the isostructural compound ZrNiSn, the essential features of the band structure of NdBiPt are derived from that of the binary substructure compound NdBi. The semimetallic nature arises from an overlap of the highest-lying anionic valence band derived from hybridized bismuth *s* and *p* states with the  $t_{2g}$  orbital derived from the Nd *d* states, but the amount of overlap is substantially reduced with respect to that of NdBi due to the presence of the transition metal. The present results on NdBiPt show that ternary intermetallics possessing the MgAgAs structure can support high carrier mobilities and low carrier densities and that the addition of a late transition-metal element into a III-V-type substructure can separate the bands near the Fermi level by as much as several hundred meV. In this regard it is interesting to speculate on the possibility of beginning with other binary rocksalt or zinc-blende substructures, e.g., InSb, GaAs, or PbTe, and inserting a transition metal to form the MgAgAs structure. If such structures are stable, this approach could provide an alternative and convenient method of tailoring the band gap of semiconductors.

## ACKNOWLEDGMENTS

Ames Laboratory is operated by the U.S. Department of Energy by Iowa State University under Contract No. W-7405-Eng-82. This work was supported by the Director of Energy Research, Office of Basic Energy Sciences.

- <sup>1</sup>S. Jin, T. H. Tiefel, M. McCormack, R. A. Fastnacht, R. Ramesh, and L. H. Chen, *Science* **264**, 413 (1994).
- <sup>2</sup>M. McCormack, S. Jin, T. H. Tiefel, R. M. Fleming, J. M. Phillips, and R. Ramesh, *Appl. Phys. Lett.* **64**, 3045 (1994).
- <sup>3</sup>H. L. Ju, C. Kwon, Q. Li, R. L. Greene, and T. Venkatesan, *Appl. Phys. Lett.* **65**, 2108 (1994).
- <sup>4</sup>T. Caillat, A. Borshchevsky, and J.-P. Fleurial, in *Proceedings of the XIIIth International Conference on Thermoelectrics*, edited by B. Mathiprakasam and P. Heenan (AIP, New York, 1995), p. 31.
- <sup>5</sup>D. J. Singh and W. E. Pickett, *Phys. Rev. B* **50**, 11 235 (1994).
- <sup>6</sup>D. T. Morelli, T. Caillat, J.-P. Fleurial, A. Borshchevsky, J. Vandersande, B. Chen, and C. Uher, *Phys. Rev. B* **51**, 9622 (1995).
- <sup>7</sup>F. G. Aliev, N. B. Brandt, V. V. Kozyr'kov, V. V. Moshchalkov, R. V. Skolozdra, Yu. V. Stadnyk, and V. K. Pecharskii, *Pis'ma Zh. Eksp. Teor. Fiz.* **45**, 535 (1987) [*JETP Lett.* **45**, 684 (1987)].
- <sup>8</sup>F. G. Aliev, A. I. Belogorokhov, N. B. Brandt, V. V. Kozyr'kov, R. V. Skolozdra, and Yu. V. Stadnyk, *Pis'ma Zh. Eksp. Teor. Fiz.* **47**, 151 (1988) [*JETP Lett.* **47**, 184 (1988)].
- <sup>9</sup>F. G. Aliev, *Physica B* **171**, 199 (1991).
- <sup>10</sup>R. Kuentzler, R. Cad, G. Schmerber, and Y. Dossmann, *J. Magn. Mater.* **104-107**, 1976 (1992).
- <sup>11</sup>P. Villars and L. D. Calvert, *Pearson's Handbook of Crystallographic Data* (AMS International, Materials Park, OH, 1991), Vol. 1, p. 137.
- <sup>12</sup>P. C. Canfield, J. D. Thompson, W. P. Beyermann, A. Lacerda, M. F. Hundley, E. Peterson, Z. Fisk, and H. R. Ott, *J. Appl. Phys.* **70**, 5800 (1991).
- <sup>13</sup>R. Movshovich, A. Lacerda, P. C. Canfield, J. D. Thompson, and Z. Fisk, *Phys. Rev. Lett.* **73**, 492 (1994).
- <sup>14</sup>Z. Fisk, P. C. Canfield, W. P. Beyermann, J. D. Thompson, M. F. Hundley, H. R. Ott, E. Felder, M. B. Maple, M. A. Lopez de la Torre, P. Visani, and C. L. Seaman, *Phys. Rev. Lett.* **67**, 3310 (1991).
- <sup>15</sup>S. Ögüt and K. M. Rabe, *Phys. Rev. B* **51**, 10 443 (1995).
- <sup>16</sup>R. A. Robinson, A. Purwanto, M. Koghi, P. C. Canfield, T. Kamiyama, T. Ishigaki, J. W. Lynn, R. Erwin, E. Peterson, and R. Movshovich, *Phys. Rev. B* **50**, 9595 (1994).
- <sup>17</sup>P. C. Canfield and Z. Fisk, *Philos. Mag. B* **65**, 1117 (1992).
- <sup>18</sup>R. B. Roberts, *Philos. Mag.* **36**, 91 (1977).
- <sup>19</sup>J. M. Honig, *J. Solid State Chem.* **1**, 19 (1969).
- <sup>20</sup>A. G. Petukhov, W. R. Lambrecht, and B. Segall, *Phys. Rev. B* **50**, 7800 (1994).
- <sup>21</sup>F. Hulliger, in *Handbook on the Physics and Chemistry of the*

- Rare Earths*, edited by K. A. Gschneidner, Jr. and L. Eyring (North-Holland, Amsterdam, 1979), Vol. 4, p. 173.
- <sup>22</sup>S. J. Allen, Jr., N. Tabatabaie, C. J. Palmstrøm, G. W. Hull, T. Sands, F. Derosa, H. L. Gilchrist, and K. C. Garrison, *Phys. Rev. Lett.* **62**, 2309 (1989).
- <sup>23</sup>S. J. Allen, Jr., N. Tabatabaie, C. J. Palmstrøm, S. Mounier, G. W. Hull, T. Sands, F. Derosa, H. L. Gilchrist, and K. C. Garrison, *Surf. Sci.* **228**, 13 (1990).
- <sup>24</sup>S. J. Allen, Jr., F. Derosa, C. J. Palmstrøm, and A. Zrenner, *Phys. Rev. B* **43**, 9599 (1991).